Coherent Microwave Emission from an Electron-hole Plasma*

Abstract: Coherent microwave radiation, 6.5 to 44 GHz, is generated by InSb at 77 °K with an injected electron current transverse to a magnetic field. The maximum output power is about 10 microwatts for input power levels of one to five watts. Grooves cut into the Suhl surface of the rod-shaped InSb samples impose the coherence and determine the frequency range of coherent operation. Wavelength measurements of a surface wave show that the effective groove width is equal to about a half-wavelength. A theory of double-stream interaction in a thin plasma layer with a magnetic field transverse to the current flow predicts instabilities in the observed frequency range. The theory predicts all of the qualitative and several of the quantitative features of the observed emission. Noise emission is predicted and observed at temperatures up to room temperature with appropriate onset magnetic fields. The theoretical analysis and concurrent experimental evidence demonstrate the existence of an instability in a thin-layer plasma in the absence of a magnetic field at 77 °K.

Introduction

Microwave noise emission from InSb was first observed by Larrabee and Hicinbothem. Such radiation, which has subsequently been observed under a variety of conditions, is generally classified as low-field or high-field emission with associated applied electric fields of the order of several volts/cm or several hundred volts/cm, respectively. This paper deals with the high-field emission produced when electrons are injected into p-InSb. It is shown that surface irregularities can suppress the noise emission and replace it with a narrow emission line. The frequency range of coherent operation is determined by the width of the surface groove. Evidence is presented which indicates that two-stream interactions play a role in the high-field emission.

Experimental details

The basic experimental arrangement is comprised of a microwave system and a voltage-pulse circuit for the InSb samples. The microwave system consists of a shorted-waveguide sample housing and a microwave receiver. A rod-shaped sample is mounted as an inductive post in the waveguide. As an alternative to the use of a waveguide sample housing, the samples were inserted into a stripline sample housing.

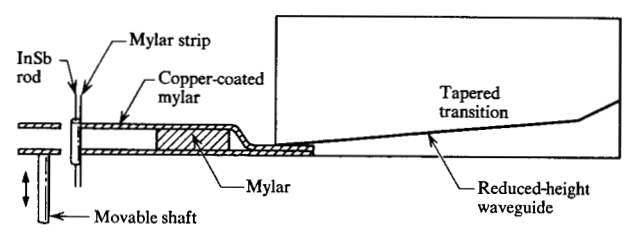


Figure 1 Schematic drawing of double stripline sample housing.

A double stripline system is used to measure the wavelength of an electrokinetic wave generated on the Suhl surface of the rod-shaped samples. The double stripline system, as shown in thes chematic drawing in Fig. 1, consists of an X-band waveguide with a tapered transition and two strips of 1-mil-thick Mylar which are coppercoated on both surfaces. At one end the two strips are squeezed together and inserted into a reduced-height waveguide. Near the opposite end a square hole in each strip is lined up to receive a rod of InSb, which passes through both holes. One stripline is fixed in position and the other is flexible. A rod, whose position is controlled by a drive screw, is placed against the flexible stripline and moves the stripline as the drive screw is turned. The power received by the striplines from two points on the sample travels back to the waveguide where the fields interfere, constructively or destructively. Thus

Sthe research reported in this paper was sponsored by the Air Force Systems Command, Rome Air Development Center, Griffiss Air Force Base. New York.

The authors are with the RCA Laboratories, Princeton, New Jersey.

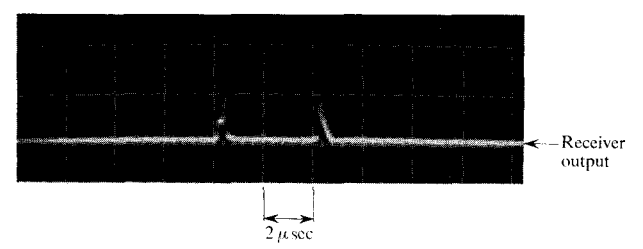
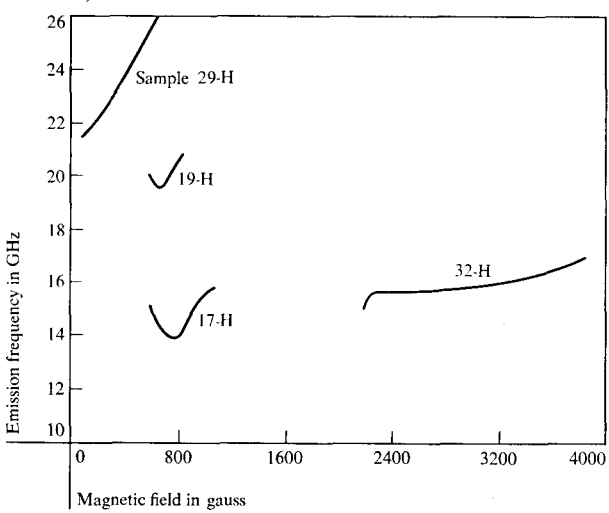


Figure 2 Receiver output from sample 17-H after surface groove, 1.3×10^{-2} mm wide and 0.9×10^{-2} mm deep, has been cut. Frequency = 13.6 GHz, B = 560 G, $\theta = 62^{\circ}$ and I = 0.11 A.

Figure 3 Emission frequency as a function of magnetic field for four samples: 17-H, $\theta = 60^{\circ}$, I = 0.092A; 19-H, $\theta = 45^{\circ}$, I = 0.095A; 29-H, $\theta = 90^{\circ}$, I = 0.062A; 32-H, $\theta = 86^{\circ}$, I = 0.1A.



the net output power should fluctuate sinusoidally as the two striplines are moved closer together. The distance traveled by the flexible stripline as the output power varies from minimum to minimum is equal to one wavelength of the electrokinetic wave.

The experiments were performed with p-type indium antimonide rods. The rod-shaped samples are typically 0.5 mm long and 0.2 mm \times 0.17 mm in cross section. Either ohmic contacts made with an indium-cadmium alloy or electron-injecting contacts made with a gallium-indium-tellurium alloy are placed at each end of the rod.

Experimental results

• Influence of surface structure on the coherent emission A wire saw was used to cut a groove in the smooth lateral surfaces of two samples, 17-H and 19-H, which were cut from an ingot of InSb containing a p-type impurity

concentration of $3 \times 10^{14} \text{ cm}^{-3}$. Prior to cutting the groove, injected current flow along either smooth surface resulted in microwave noise. The grooves, which are aligned perpendicular to the current flow, are 1.3×10^{-2} mm wide and 0.9×10^{-2} mm deep. With the current flow along the grooved surface, coherent emission at frequencies from 10 to >22 GHz is generated in sample 17-H and from 18 to 30 GHz in sample 19-H. The emission, as shown in Fig. 2 for sample 17-H, is relatively noisefree. A double-peaked response is observed because the emission frequency decreases with time and the receiver responds to two frequencies.² One is the sum of the local oscillator frequency and the intermediate frequency and the other is the difference of these two frequencies. The lower of the resultant frequencies corresponds to the dial setting. The instantaneous output power from samples 17-H and 19-H is about 5 μ W for instantaneous input power of 1.5 W.

Numerous additional samples, cut from the same ingot, were tested in the single and double stripline sample housings. A groove 2.5×10^{-2} mm wide was cut on the smooth lateral surface of each of three samples, and all three samples emitted coherent power in the frequency range from 6.5 to 11 GHz. Grooves 1.3×10^{-2} mm wide were cut in the remaining samples. The output frequencies of the samples with the narrower grooves were between 16 and 30 GHz. These experiments provide substantial confirmation that the groove is instrumental in imposing the coherence and that it also determines the approximate frequency.

• Dependence of frequency on experimental parameters The frequency of emission from the grooved samples normally decreases with time during the pulse and therefore frequency measurements as a function of a particular parameter are made at a given time after the pulse initiation. Measurements of frequency as a function of magnetic field have certain general features, as shown in Fig. 3 for four different samples. At high magnetic fields (>2000 G) the frequency is almost independent of field. At moderate magnetic fields (500 to 2000 G) the frequency increases with magnetic field above 900 G and has a minimum with respect to field at 700 to 900 G. An alternative frequency dependence, as exhibited by sample 29-H, is also possible. In that case the emission is observed with an applied magnetic field of only 50 G. As the magnetic field is increased from 50 G to 600 G, the frequency increases by 20%.

The frequency decreases with increasing injected current (di/dI < 0). In a transverse magnetic field the injected current is usually a small fraction of the total current and the I-V characteristic appears almost linear. In a few samples such as 19-H the injected current is an appreciable fraction of the total current and a quan-

titative measurement of the dependence of frequency on injected current is possible.

The decrease of emission frequency with time is caused by lattice heating at the Suhl surface where the current density is highest. This is substantiated by observation of a frequency decrease at a given time after pulse initiation as the ambient temperature is raised by increasing the pulse repetition rate.

The dependence of frequency on the angle θ , formed by the electric and magnetic fields, lacked consistency from sample to sample.

Wavelength measurements

Experiments were performed to determine the nature of the wave generated in indium antimonide during the emission process. The double stripline sample housing described in the previous section was used to measure the wavelength of this electrokinetic wave. Wavelength measurements were made on two samples, 31-H and 32-H, each with 3×10^{14} p-type impurities/cm³ and a 2.5×10^{-2} -mm-wide groove cut into one lateral surface. The frequency range of the emission for sample 31-H is 8 to 10.5 GHz and for sample 32-H is 7.2 to 8.3 GHz. The sinusoidal power variation of the output power as the striplines are moved closer together is, typically, 10×10^{20} of the total output power. The measured phase velocities vary from 4.6×10^{7} cm/sec to 10^{8} cm/sec at applied electric fields from 330 V/cm to 700 V/cm.

• Critical hole density

Samples with various p-type impurity concentrations were tested to determine the effect on the microwave generation mechanism of altering the hole density. Tests were conducted on grooved samples with nominal impurity concentrations of 1.5×10^{15} , 4×10^{14} , 3×10^{14} and $1 \text{ to } 2 \times 10^{14}$ impurities/cm³. All samples, except those cut from the wafer with 3×10^{14} impurities/cm³, are oriented such that the grooved surface is parallel to the $\langle 100 \rangle$ crystallographic plane. With moderate electron injection, coherent microwave power is generated in most samples from each impurity group except those with concentrations of 1 to $2 \times 10^{14}/\text{cm}^3$, which do not emit coherent power or noise. The experiments demonstrate that a critical hole density of about $2 \times 10^{14}/\text{cm}^3$ must be exceeded in order to generate an instability.

A sample with 1.5×10^{15} impurities/cm³ generated coherent emission at frequencies as high as 44 GHz. The sample surface was not grooved but had etch pits of various widths.

• Critical magnetic field at high current injection

Experiments were performed on several samples to determine the critical magnetic field which is required for emission onset under the condition of equal charge carrier density. This condition is achieved by high current injection into pure material. High injection contacts made from In-Ga-Te alloy were soldered to one end of each of several samples which have an impurity concentration of 1 to $2 \times 10^{14}/\text{cm}^3$. Ohmic contacts were placed on the opposite end. In zero magnetic field, current injection begins at applied potentials of 0.25 to 2 volts across a 0.7-mm-long sample. A groove 1.3×10^{-2} mm wide and 1.3×10^{-2} mm deep was cut into a lateral surface of one of these samples, 7-L. This sample emits coherent power at K-band frequencies for magnetic field values greater than 1600 G.

Tests were also performed on samples 16-L and 17-L, which do not have surface grooves. The electron injection into sample 16-L is greater than that for sample 17-L, although the injection into both is high. For sample 16-L the critical transverse magnetic field for noise emission from one Suhl surface is 1300 G and from the opposite surface it is 1420 G. For sample 17-L, where the injection current is less, the critical transverse field for noise emission is 2000 G when the current flow is along the single clean Suhl surface. Thus, with high current injection at $T = 77^{\circ}$ K, emission is observed only when $B_{\perp} > 1300$ G.

An experiment to determine the critical magnetic field in the intrinsic conduction region was performed at $T=287^{\circ}\mathrm{K}$. At this elevated temperature C-band noise emission is generated by a sample in a 13.2-kG transverse magnetic field. The required electric field is 300 volts/cm. The noise emission is just above the receiver noise level, which is about $-80~\mathrm{dBm}$.

Theory

When electrons are injected into a bar of p-InSb in the presence of a transverse magnetic field, the Lorentz force pushes the injected plasma into a thin layer along one surface of the sample via the Suhl effect.³ The slow waves that such a thin plasma layer can support have been studied with the aid of the two-fluid electron-hole model, the quasistatic approximation and the assumption of a homogeneous layer.⁴ We conclude that the layer can support waves which consist of propagating dipolar surface-charge disturbances as illustrated in Fig. 4. The pertinent dispersion relation is

$$1 + \sum_{a} \frac{\omega_{pa}^2 \Omega_a}{(\omega - k v_{oa})(\omega_{ca}^2 - \Omega_a^2)} \approx 0, \tag{1}$$

where

$$\Omega_a = \omega - k v_{oa} - i \nu_a,$$

the summation is over electrons and holes, $\omega/2\pi$ ($\equiv f$) is the active frequency of the system, and k is the wave number. Each species a is characterized by a steady-state drift velocity v_{oa} , a collision frequency v_a , a steady-state density n_{oa} , a charge per carrier q_a , a plasma frequency

603

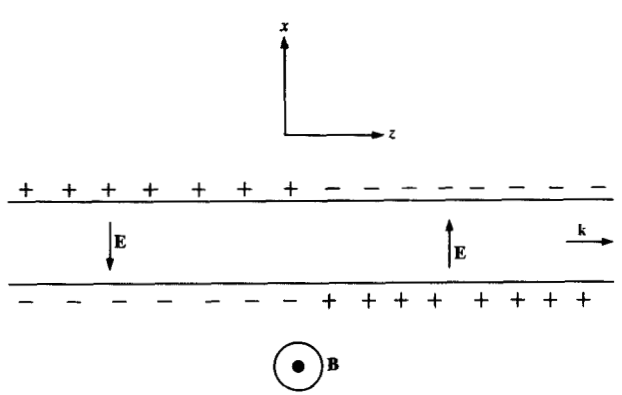
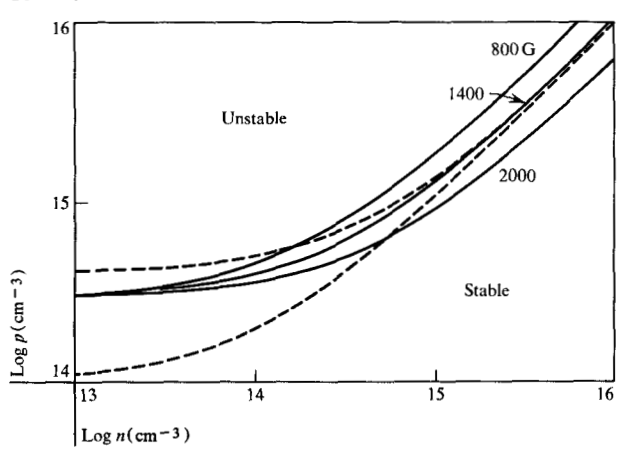


Figure 4 Dipolar thin-layer wave-configuration.

Figure 5 Instability onset conditions at 77°K. The solid curves separate stable and unstable regions for various values of magnetic field. The dashed curves show the injection level $p = p_a + n$, for $p_a = 10^{14}$ cm⁻³ and 4×10^{14} cm⁻³. The parameters appropriate for 77°K are $m_h = 0.5$ m₀, $v_h = 3.5 \times 10^{11}$ sec⁻¹, $m_e = 0.015$ m₀ and $v_e = 5.8 \times 10^{11}$ sec⁻¹.



 $\omega_{pa} = (n_{oa}q_a^2/\epsilon_L m_a)^{\frac{1}{2}}$, and a cyclotron frequency $\omega_{co} = q_a B/m_a$. This dispersion relation reveals that these thinlayer dipolar waves can experience two-stream instability, when the electrons drift with respect to the holes, in a manner completely analogous to the classical two-stream interaction involving bulk-space-charge waves. The subject of two-stream interaction in semiconductors was recently reviewed in Ref. 5.

The dispersion relation (1) has two unstable roots. One is dominant at high magnetic fields, $B \gtrsim 600$ G in InSb at 77°K, and the other is dominant at low fields. The latter root could exist with no magnetic field if a thin layer were provided without the aid of the Suhl effect. Since most of our data involves B > 600 G, we concentrate on the high-field mode. It can be shown, with the aid of approximations valid under most of the

pertinent experimental condition reported in this paper, that the high-field mode has an onset condition⁶

$$1 - \frac{\omega_{ph}^2}{\nu_h^2} + \omega_{pe}^2 \frac{[\omega^2 - \nu^2]}{[\omega^2 + \nu^2]^2} < 0.$$
 (2)

This onset condition is plotted in bold lines in Fig. 5 using parameters⁷⁻¹⁰ appropriate for InSb at 77°K for three different values of magnetic field. The dashed lines represent steady-state density conditions, which one could obtain by injecting electrons into p-material of two different ambient densities. The onset conditions indicate two critical parameters. The ambient density of the p-InSb must exceed a critical value, $\approx 3 \times 10^{14}$ cm⁻³, in order to have instability with low injection. Under high injection conditions, $p \approx n$, the magnetic field must exceed a critical value, ≈ 1400 G. The critical magnetic field required when n = p increases with temperature via the hole collision frequency, reaching a predicted value of 11,000 G at room temperature. This prediction is based on a room temperature hole collision frequency of $2 \times 10^{12}/\text{sec.}^{11}$

A general discussion of the dispersion relation (1) must rest on computer solutions, but the nature of such solutions can be illustrated with analytical expressions that are valid in the immediate vicinity of instability onset. 6 In this region the frequency of maximum gain is

$$\omega_{\max} \approx \frac{1}{\sqrt{2}} \left\{ \frac{\omega_{ph}^2}{\left[1 + \omega_{pe}^2 \frac{(\omega_{pe}^2 - \nu_e^2)}{(\omega_{ce}^2 + \nu_e^2)^2}\right]} - \nu_h^2 \right\}^{\frac{1}{2}}$$
(3)

and the frequency associated with a given wave number k is

$$\omega \approx \frac{k v_{oe}}{1 + \frac{v_h \omega_{pe}^2 v_e}{\omega_{ph}^2 (\omega_{ce}^2 + v_e^2)}}.$$
 (4)

The surface groove is effecting coherence by selecting a given value of k, but work must be done when there is gain, $\omega \approx \omega_{\max}$.

Since the theoretical model simulates the very inhomogeneous Suhl layer with a homogeneous plasma layer, one can expect only qualitative agreement with experiment for predictions that are sensitive to the steady-state plasma density. For the case of low injection into p-InSb at 77°K with $p\approx 3$ to 4×10^{14} cm⁻³, $\omega_{\rm max}\approx 25$ GHz. Higher density *p*-material should generally operate at higher frequencies. Thus the predicted frequency range is consistent with experiment.

Discussion

In light of the experiments and theory presented in previous sections, the microwave generation mechanism in indium antimonide can be explained in terms of a doublestream interaction in a thin plasma layer. In the experiments this layer is produced by the transverse magnetic field component's forcing the injected current stream against a lateral surface, which is referred to as the Suhl surface. The analysis of the double-stream interaction in a thin plasma layer predicts instabilities in the observed frequency range with properties in the following areas that are in excellent agreement with the experimental results: (1) critical doping density and magnetic field associated with instability onset, (2) phase velocity of the surface plasma wave, (3) output frequency as a function of the transverse magnetic field, and (4) output frequency as a function of injection current.

The calculated hole and electron densities at the onset of instability for various magnetic field values are shown in Fig. 5. The experimental results confirm certain values on the curves, in particular, the onset hole density at low electron-injection level and the minimum magnetic field at a high electron-injection level. The general lack of emission from samples with impurity concentrations of 1 to 2 \times 10¹⁴/cm³ and low or moderate electron injection, and the copious emission from samples with impurity concentrations equal to or greater than 3×10^{14} cm³ and about the same level of electron injection, is direct evidence that there is a critical value of the hole density, which is between 2 and $3 \times 10^{14}/\text{cm}^3$. This experimental value is in excellent agreement with the onset hole density of $3 \times 10^{14}/\text{cm}^3$ predicted by the theory for low electron densities.

The analysis indicates, as illustrated in Fig. 5, that a rod of InSb with a subcritical ambient hole density can generate microwave power if the injection current is high and $B \ge 1400$ G. Samples 7-L, 16-L and 17-L with a subcritical ambient hole density emit power when the current injection level is high and $B \ge 1300$ G. The critical magnetic field increases with increasing temperature, reaching a value of 13,200 G at $T = 287^{\circ}$ K. The theory predicts such a rise of the critical field with temperature and indicates a critical field of 11,000 G at room temperature.

The measurements of the wave phase velocity v_{ph} yield values that are approximately equal to the electron drift velocity v_{oe} obtained by extrapolation of the Glicksman and Hicinbothem data. The measurements were made at high magnetic fields where the dispersion relation (4) reduces to

$$v_{oe} = \omega/k \equiv v_{ph}$$
.

Thus the measured phase velocity is in agreement with the calculated value.

In light of the theory, the groove experiments together with the wavelength measurements suggest that the presence of the groove causes a resonance in the charge carrier streams. Power reflection in the current stream, which is caused by direction changes around the groove,

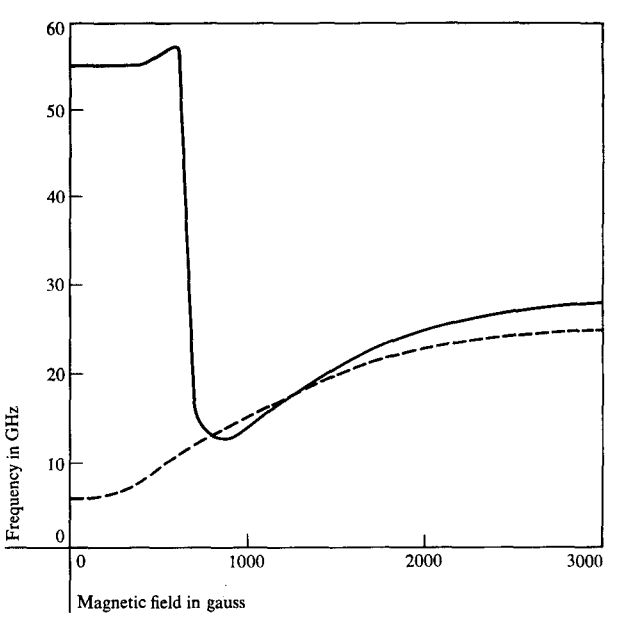


Figure 6 Theoretical prediction of frequency as a function of magnetic field—computer solutions of the exact dispersion relation for the frequency of maximum gain (solid curve) and for the frequency associated with a wavelength of 2.5×10^{-8} cm (dashed curve). These results are for the conditions $p_a = 4 \times 10^{14}$ cm⁻⁸, $n = 10^{14}$ cm⁻⁸ and $T = 77^{\circ}$ K.

could initiate an oscillation under the groove. Once the oscillation is established, a wave pattern can form along the entire length of the sample. The frequency of oscillation is largely determined by the groove width W, as shown in the experiments.

The most stable operation should occur when half the wavelength of the maximum-gain frequency matches the effective groove width. In the experimental procedures we assume that the various parameters are adjusted so that this matching condition is generally in effect. The analysis indicates that parameters can be varied over a range of values without changing the matching condition, as evidenced by the results of the computer solution shown in Fig. 6, where the maximum-gain frequency and the frequency with a fixed wavelength or constant k-vector are plotted as functions of magnetic field. However, as the range of parameter values is extended, the matching condition is not satisfied and the oscillation frequency is either near the maximum-gain frequency or the resonant-groove frequency or, more often, the oscillation ceases.

The measured values of f vs. B for four different samples, as shown in Fig. 3, are in good qualitative agreement with the theory. For experiment and theory, with 900 G < B < 2000 G, the oscillation frequency increases with increasing magnetic field; at B > 2000 G the frequency

is relatively independent of the magnetic field. The theory shows that, as the magnetic field decreases below 900 G, the maximum-gain frequency, Eq. (3), exhibits a minimum when $\omega_{ce}^2 \approx 3v_e^2$, which corresponds to $B \approx 800$ G at 77°K. The frequency with a constant k-vector or resonant-groove frequency, Eq. (4), continues to decrease with decreasing field. The frequency minimum occurs at a calculated magnetic field value that is independent of the surface carrier densities, and can therefore be quantitatively compared with the experiments. Samples 17-H and 19-H exhibit this minimum at magnetic fields between 700 and 900 G, which compare with calculated values of about 800 G. The emission cuts off at magnetic field values between 500 and 600 G where the maximum-gain frequency diverges from the resonant frequency of the groove. A low magnetic field mode of operation is illustrated by data for sample 29-H. The existence of this mode is consistent with the theoretical prediction of instability for low magnetic field in a thin-layer plasma. Below 50 G the magnetic field is not sufficient to produce the thin plasma layer at the lateral surface; damping effects dominate and the oscillation ceases.

To complete the confirmation of the theory by the experimental observations, the theory must predict the dependence of frequency on injected electron current. The theoretical results expressed in Eq. (4), which show df/dn < 0 for $k = \pi/W = \text{constant}$, agree qualitatively with the experimental results, which show $df/dI_- < 0$, if one assumes reasonably that $n \propto I_-$.

An onset value of electric field is another characteristic of the high-field emission observed from InSb. The current form of the theory, which uses the free plasma boundary conditions,⁴ does not predict an onset field. Application of boundary conditions that more nearly represent the conditions at a semiconductor surface will introduce additional thermal effects into the dispersion relation and will result in an onset drift velocity. It seems reasonable to assume that the drift velocity must approach the electron thermal velocity, which would require a field of the order of 100 V/cm.

References

- R. D. Larrabee and W. A. Hicinbothem, Jr., Effects de Plasmas Dans Les Solides, Dunod, Paris, 1965, pp. 181 to 187.
- G. A. Swartz and B. B. Robinson, Appl. Phys. Letters 9, 232 (1966).
- 3. W. Shockley, Electrons and Holes in Semiconductors, D. Van Nostrand, Co., Inc., Princeton, N. J. 1950.
- B. B. Robinson and B. Vural, RCA Review 29, 270 (1968).
- 5. B. Robinson, Proceedings of the CCNY Conference on Wave Interactions in Solids, Department of Electrical Engineering, City University of New York (1969); to be published in IEEE Trans. Electron Devices ED-17 (1970).
- 6. G. A. Schwartz and B. B. Robinson, to be published in J. Appl. Phys. 40 (1969).
- 7. D. M. S. Bagguley, M. L. A. Robinson and R. A. Stradling, *Phys. Letters* 6, 143 (1963).
- 8. E. H. Putley, Proc. Phys. Soc. 73, 128 (1959).
- E. D. Palik, G. S. Picus, S. Teitler and R. F. Wallis, Phys. Rev. 122, 475 (1961).
- M. Glicksman and W. A. Hicinbothem, Jr., Effets de Plasmas Dans Les Solides, Dunod, Paris 1965, pp. 137 to 146.
- 11. V. G. Zolotarev and D. N. Nasdedov, Soviet Phys.-Solid State 3, 2400 (1962).

Received April 14, 1969